Inorganica Chimica Acta, 150 (1988) 249–256

Electrochemistry and Spectroelectrochemistry of a Linear Triiron Cluster

JUDITH R. FISH, TADEUSZ MALINSKI*

Department of Chemistry, Oakland University, Rochester, Mich. 48309 - 4401, U.S.A.

ARMIN J. MAYR and KEITH H. PANNELL

Department of Chemistry, University of Texas at El Paso, El Paso, Tex. 79968, U.S.A.

(Received March 29, 1988)

Abstract

This work reports electrochemical and spectroelectrochemical studies of a unique linear triiron cluster carbonyl complex, $Fe_3(CO)_7L_2$, where L is an α-diazothioketone. Oxidation and reduction reactions have been observed in non-aqueous media over the temperature range −40 to 20 °C by differential pulse voltammetry, cyclic voltammetry, thin-layer, UV–Vis spectroelectrochemistry and ESR spectrometry. The sequence of the individual electron-transfer steps comprising the overall redox process is described, and a comparison between the electrochemistry of different non-linear iron–carbonyl complexes is discussed. A single one electron reduction produces the radical anion, $[Fe_3(CO)_7L_2]^{\cdot-}$, which decomposes at temperatures greater than −10 °C to species which are reduced at a more negative potential, an ECE mechanism. A single one-electron oxidation produces the radical cation, $[Fe_3(CO)_7L_2]^{+\cdot}$, which is unstable, decomposing completely at room temperature, an EC mechanism. Spectroscopic evidence indicates that in non-bonding solvents, the $Fe_3(CO)_7L_2$ framework remains intact at low temperatures for both the anion and cation radical produced electrochemically with radical stability higher than might be expected for a linear structure. Observations indicate only strongly bonding solvents disrupt the structure. Low temperature stability occurs at relatively high temperatures, with the cation radical less stable and vulnerable to strongly bonding solvents.

Introduction

Chemical activation of π-heterocycles resulting from complexation to transition metal complexes tends not to be investigated due to the general observation that the hetero atoms present often result in simple σ-bonding which seldom proceeds to further chemical reactivity [1] During the past several years, a striking pattern of reactivity has been established for a specific class of heterocycle, the thia or selena diazoles, which exhibit a wide range of chemical reactivity predicated upon the presence of transition metal complexes [2–6]. The pattern of reactivity as outlined in Scheme 1, appears to be derived from an initial metal-promoted ring opening of the diazoles to transient α-diazothio a seleno ketone [7], which are then stabilized by complexation to metal centers via the S(Se) or N atoms. It has been shown a portion of the complexes containing metal produced may be readily removed via mild oxidation, e.g. with trimethylamine oxide, to yield a nascent organic fragment for further study [8]. A knowledge of the redox processes and products involved would help in understanding the mechanism of the fragmentations which occur in these systems. This work reports electrochemical and spectroelectrochemical studies of a unique linear triiron cluster complex, $Fe_3(CO)_7L_2$, where L is an α-diazothioketone, the unifying species in Scheme 1, [7]. The structure of the complex is shown in Fig. 1. The intrinsic redox properties of

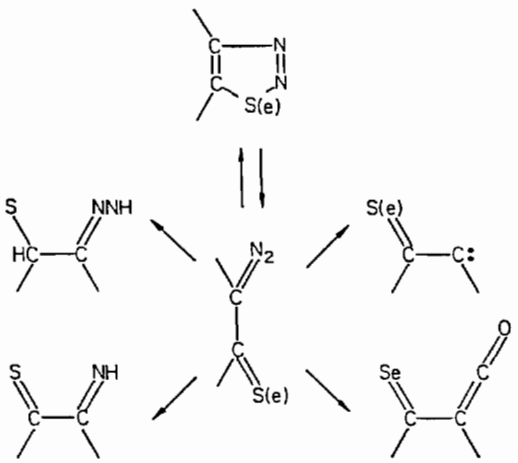

Scheme 1.

*Author to whom correspondence should be addressed.

0020-1693/88/$3.50

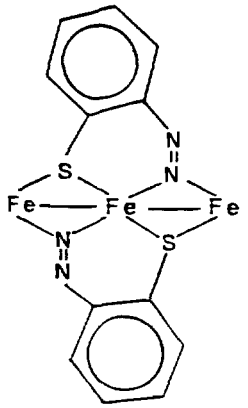

Fig. 1. Structure of linear triiron cluster.

the linear triiron system have not been observed previously as other known Fe_3 complexes are observed to be triangular.

Experimental

Linear triiron cluster, $Fe_3(CO)_7L_2$, was prepared from $Fe_2(CO)_9$ and 1,2,3-benzothiadiazole in hexane by the procedure published previously [7]. $Fe(CO)_5$ and $Fe_3(CO)_{12}$ (Strem Chemicals) were purified by distillation or sublimation *in vacuo*. Methylene chloride, CH_2Cl_2, (Fisher Scientific) technical grade, was twice distilled from P_2O_5, and stored in the dark over activated 4 Å molecular sieves. Acetonitrile, CH_3CN (Matheson Coleman and Bell), and dimethylacetamide, DMA, (Fisher Scientific), were all received as reagent grade from the manufacturer and dried over 4 Å molecular sieves prior to use. Dimethyl sulfoxide, Me_2SO (Eastman Chemical) was purified by fractional crystallization using a method similar to that described for purification of pyridine [9]. For all electrochemical experiments, the solvents contained 0.1 M tetrabutylammonium perchlorate (TBAP) as supporting electrolyte. TBAP was recrystallized and dried *in vacuo* prior to use.

A platinum disk served as the working electrode and a platinum wire as the auxiliary electrode for conventional cyclic voltammetric and differential pulse voltammetric measurements. A saturated calomel electrode (SCE), separated from the bulk of the solution by a fritted glass disk, was used as the reference electrode. Cyclic voltammetric measurements were made using a conventional three-electrode configuration and an IBM Model EC 225 voltammetric analyzer. Current–voltage curves were collected on a Houston Instruments Omnigraphic X-Y recorder at scan rates from 0.05 to 0.30 Vs^{-1} and on a Tektronix 511 oscilloscope at scan rates from 0.5 to 10 Vs^{-1}. For controlled-potential coulometry and controlled-potential electrolysis, a Princeton Applied Research Model 173 potentiostat was used. UV–Vis spectra were obtained with a Tracor Northern optical multichannel analysis system. The system was composed of a Tracor Northern 6050 spectrometer containing a crossed Czerny-Turner spectrograph in conjunction with the Tracor Northern 1710 multichannel analyzer. Each spectrum results from the signal averaging of 100 5-ms spectral acquisitions. Each acquisition represents a single spectrum from 295 to 920 nm, simultaneously recorded by a double-array detector with a resolution of 1.2 nm/channel. ESR spectra were recorded during *in situ* electrolysis on an IBM Model ER100D spectrometer, equipped with ER 040-X microwave bridge and an ER 080 power supply, or on a Varian Model E-104 spectrometer. Low-temperature ESR spectral measurements were achieved with a Varian variable-temperature controller, which monitors the temperature from 0 to −150 °C. The g values were measured relative to diphenylpicrylhydrazyl (DPPH) (g = 2.0036 ± 0.0003). UV–Vis spectroelectrochemistry was performed both in a bulk cell and in a thin-layer cell. The bulk cell followed the design of Fajer *et al.* [10] and had an optical path length of 0.19 cm. The thin-layer cell had a 1000-Lpi gold minigrid working electrode sandwiched between two glass slides and a platinum-gauze auxiliary electrode [11] In both cases, the SCE was separated from the rest of the solution by a fritted bridge containing supporting electrolyte and solvent. ESR spectroelectrochemistry was performed in microcell and the design followed that of Bagchi *et al.* [12].

Results and Discussion

Voltammetry of $Fe_3(CO)_7L_2$ in CH_2Cl_2

Figure 2a illustrates a typical differential pulse voltammogram for the oxidation and reduction of $Fe_3(CO)_7L_2$ in CH_2Cl_2 (0.1 M TBAP) on a rotating platinum disk electrode. As seen in this Figure, two processes occur in differential pulse voltammetry: an oxidation at $E_{1/2}$ = 0.81 V (peak I) and a reduction at $E_{1/2}$ = −0.88 V (peak II). The currents observed for the two peaks are equal in height. Half current peak widths are 95 ± 2 mV for the oxidation process and 97 ± 2 mV for the reduction process. These values are close to that predicted for a reversible one electron transfer reaction (93 mV for pulse amplitude 25 mV) and indicate that both electrode processes are mass transport controlled [13].

A typical cyclic voltammogram of $Fe_3(CO)_7L_2$ obtained in CH_2Cl_2 at 20 °C is shown in Fig. 2b. In the range of potential between 0.0 and 1.4 V, one oxidation peak (peak Ia in Fig. 1b) is observed in cyclic voltammetry of $Fe_3(CO)_7L_2$. The peak at E_{pa} = 0.84 has a slope $E_p - E_{p/2}$ = 60 mV indicative of reversible electron transfer. No reduction peak is observed after reversal of the anodic potential scan at

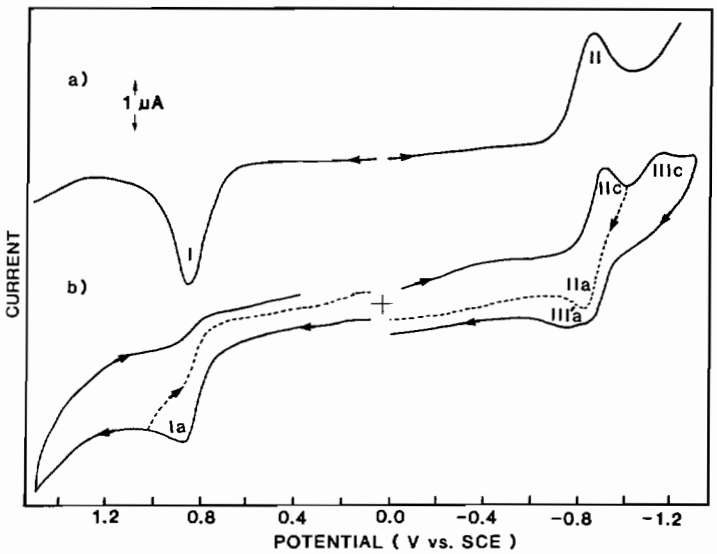

Fig. 2. Voltammetric data obtained during the electroreduction and electrooxidation of 1 mM of $Fe_3(CO)_7L_2$ in CH_2Cl_2 containing 0.1 M TBAP. (a) Differential-pulse voltammogram obtained at rotating platinum disk electrode (600 rpm) with a potential sweep rate of 5 mV s^{-1}, a pulse interval of 2 s, and a pulse amplitude 25 mV. (b) Cyclic voltammogram obtained at stationary platinum disk electrode with a potential sweep rate of 100 mV s^{-1} (temp. 25 °C).

scan rates as high as 100 mV s^{-1} following the oxidation process which indicates that the process is irreversible in the time scale of cyclic voltammetry at 20 °C and, therefore, probably involves an EC mechanism, *i.e.* the electrochemical step is followed by a chemical reaction.

In the range of potentials between 0.0 and −1.35 V *versus* SCE, two reduction peaks IIc and IIIc are obtained with continuous scan. The first process at $E_{pc} = -0.91$ V (peak IIc) has a slope $E_p - E_{p/2} = 60$ mV indicating a one electron transfer process. A reoxidation peak is observed at $E_{pa} = -0.85$ V. At the switching potential −1.35 V and potential scan rate 0.1 V s^{-1}, the ratio of the anodic to cathodic peak currents i_{pa}/i_{pc} is 0.35. This ratio increases up to 0.95 at potential scan rate 10 V s^{-1}. The current of the reoxidation process is also dependent upon switching potential. At switching potential −1.0 V, i_{pa}/i_{pc} is 0.60 of that observed at potential scan rate 0.1 V s^{-1}.

A second reduction process (IIIc) is observed at $E_{pc} = -1.16$ V with no observable reoxidation peak coupled to this process. The sum of cathodic peak current for peak IIIc and anodic current for peak IIa is approximately equal to that of cathodic current of peak IIc. Reversing the potential scan at the potential of process IIIc yields a new oxidation peak (labeled III'a) in addition to peak IIa. This peak is not observed upon reduction scans scanning to −1.35 V nor is it observed if the switching potential is more positive than the potential of the second reduction. This data indicates that peak IIIc is due to a reduction process involving the products of decomposition of the species reduced in process IIc. The product(s) of the second reduction is also unstable and probably undergoes chemical reaction to product(s) oxidized at more positive potential (peak III'a).

In order to stabilize the products of the electrochemical processes, the reduction and oxidation of $Fe_3(CO)_7L_2$ were investigated by cyclic voltammetry at low temperatures. Typical cyclic voltammograms of $Fe_3(CO)_7L_2$ obtained in CH_2Cl_2 at various temperatures are shown in Fig. 3. The current of peak IIa increases as temperature decreases. Also, a cathodic peak (Ic) coupled to the first oxidation peak, Ia,

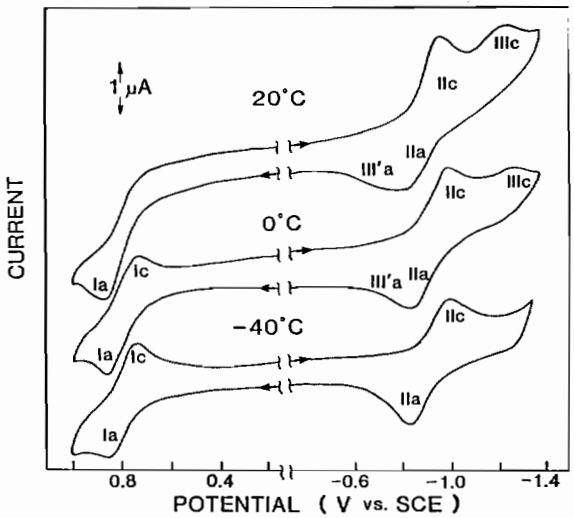

Fig. 3. Cyclic voltammograms of 1 mM $Fe_3(CO)_7L_2$ obtained at stationary platinum electrode in CH_2Cl_2 (0.1 M TBAP) solution at various temperatures.

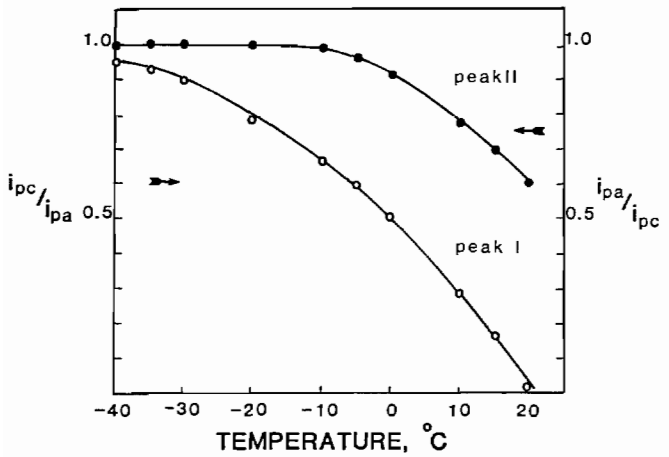

Fig. 4. Dependencies of the cyclic voltammetric peak current ratio of $Fe_3(CO)_7L_2$ in CH_2Cl_2 (0.1 M TBAP) on the temperature. Open circles: peak I; solid circles: peak II. Current was recorded at potential scan rate 0.1 V s^{-1} and a switching potential of −1.0 V.

appears. Simultaneously, peaks IIIc and III'a decrease. Ratios of cathodic to anodic peak currents for peak I and peak II *versus* temperature are plotted in Fig. 4. These data show that during the cyclic voltammetric experiment, while the product of the first reduction (process II) is reaching stability at −10 °C in CH_2Cl_2, the product of the first oxidation still undergoes decomposition at −40 °C. At potential scan rate 0.1 V s^{-1}, about 5% of the oxidation product is decomposed during 2 s of electrolysis and the process is quasi-reversible at −40 °C, whereas process II is totally reversible at −10 °C for the same electrolysis time and scan rate.

Solvent Effects on Redox Potentials

The results of the measurement of half-wave potentials for both oxidation and reduction of $Fe_3(CO)_7L_2$ in three non-aqueous solvents are summarized in Table I. The solvents in the Table are listed in terms of increasing bonding ability, which is roughly correlated with the Gutmann donor number [14]. The shapes of the differential pulse and cyclic voltammograms of $Fe_3(CO)_7L_2$ in CH_3CN are identical to that observed in CH_2Cl_2 (Fig. 2). However, in CH_3CN, the half-wave potential of oxidation peak I is shifted about 120 mV more negative; for the first reduction, (peak II) the shift is 90 mV but in the positive direction; and for the second reduction, peak III is shifted 20 mV in the negative direction. Significant shifts of the potential of waves I and II (100 and 110 mV respectively) remain after correction for liquid junction potential which, therefore, are not due to differences in junction potential between these two solvents (Table I). The dirccional property of the potential shift observed after junction potential correction, in opposite directions for wave I and II, indicates that solvent properties (donor–acceptor number and dielectric constant) influence electrochemical processes I and II with opposite effects. Probably, differences in solvation sphere or ion pair formation make oxidation process I as well as a reduction process II easier.

Spectroelectrochemistry

Electronic absorption spectra of the oxidation of $Fe_3(CO)_7L_2$ in CH_2Cl_2 (0.1 M TBAP) obtained during the thin-layer spectroelectrochemical experiment are shown in Fig. 5. The original spectrum of $Fe_3(CO)_7L_2$ shows one major peak at 355 nm with molar absorptivity of 7.5×10^3 M^{-1} cm^{-1}. Two other

TABLE I. Half-wave Potentials and Peak Potentials (V *vs.* SCE) in Selected Solvents Containing 0.1 M TBAP (scan rate 0.1 V s^{-1})

Solvent	DN[a]	Oxidation(I)				Reduction(II)				Reduction(III)				Oxidation(IV)			
		E_{pc}	E_{pa}	$E_{1/2}$	$E_{1/2}$[b]	E_{pc}	E_{pa}	$E_{1/2}$	$E_{1/2}$[b]	E_{pc}	E_{pa}	$E_{1/2}$	$E_{1/2}$[b]	E_{pc}	E_{pa}	$E_{1/2}$	$E_{1/2}$[b]
CH_2Cl_2	0.0		0.84	0.81	0.31	−0.91	−0.85	−0.88	−1.38	−1.16	−0.76[c]	−1.13	−1.63				
CH_3CN	14.1		0.72	0.69	0.21	−0.82	−0.76	−0.79	−1.27	−1.18		−1.15	−1.63				
Me_2SO	29.8		0.66	0.63	0.18	−0.70	−0.64	−0.67	−1.12	−1.14		−1.11	−1.56	0.20	0.26	0.23	−0.22

[a]Taken from ref. 14. [b]Corrected for liquid junction potential; by referring $E_{1/2}$ *vs.* SCE for triiron cluster to the $E_{1/2}$ *vs.* SCE for ferrocene/ferrocenium couple, Fc/Fc^+, *i.e.* for $MeCl_2$, CH_3CN, and Me_2SO; a value of 0.50, 0.48 and 0.45 V should be subtracted from $E_{1/2}$ *vs.* SCE of triiron cluster. [c]Peak III'a.

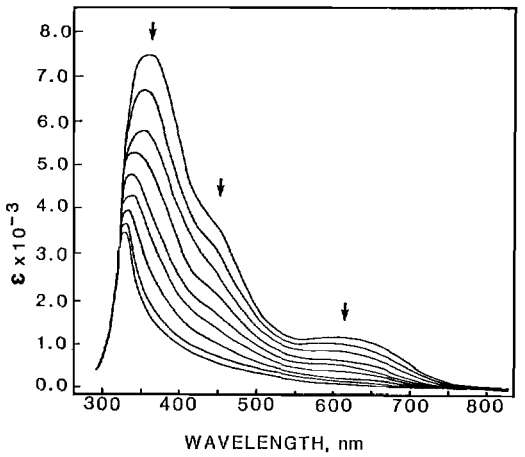

Fig. 5. Thin-layer electronic absorption spectra for oxidation of $Fe_3(CO)_7L_2$ in CH_2Cl_2 (0.1 M TBAP) at 1.15 V.

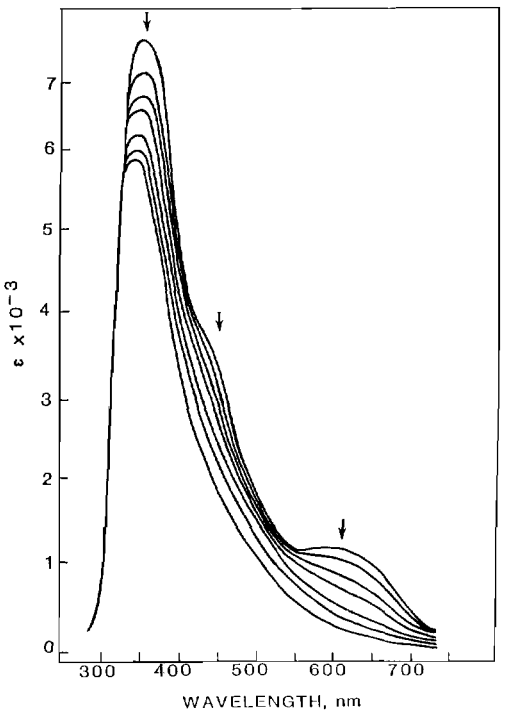

Fig. 6. Thin-layer electronic absorption spectra for reduction of $Fe_3(CO)_7L_2$ in CH_2Cl_2 (0.1 M TBAP) at −1.00 V.

small peaks are observed at 450 and 610 nm. During controlled potential electrolysis at the plateau of wave Ia at 1.15 V, the peak at 355 nm decreases to 3.3×10^3 M^{-1} cm^{-1} and is shifted to 330 nm. The peaks at 450 and 610 nm also decrease and disappear when the electrolysis is completed.

A similar change in UV–Vis spectra was observed during electrochemical reduction at −1.00 V (Fig. 6). Peaks at 450 and 610 nm are not observed after complete electrolysis. However, the decrease of the 355 nm peak is less significant than in the oxidation process (5.8×10^3 M^{-1} cm^{-1} after electrolysis). Peak wavelength is shifted 15 nm toward shorter wavelengths. Both oxidation and reduction are irreversible in the time scale of spectroelectrochemistry (about 180 s), *i.e.* neither the rereduction nor the reoxidation produces the original spectrum. This indicates that both the product of oxidation and the product of reduction are shortlived species and undergo decomposition in the time scale of the spectroelectrochemical experiment. However, the spectra indicate that the product(s) of decomposition following electrochemical oxidation is not the same as following electrochemical reduction (Figs. 5 and 6). Coulometric data obtained simultaneously with spectroelectrochemical data indicated that 1.06 and 1.02 faradays were transferred in process I and II, respectively confirming a one electron transfer process.

In order to determine the site of reduction, the products of controlled-potential electrolysis of $Fe_3(CO)_7L_2$ were investigated by ESR spectroscopy. Isotropic ESR signals were obtained at $g = 2.049$ and 2.003 (−150 °C) (Table II) after 20 s of electrolysis in the ESR cavity at −1.00 V.

TABLE II. ESR Data Obtained During Controlled Potential Electrolysis[a] of $Fe_3(CO)_7L_2$ in CH_2Cl_2 (0.1 M TBAP)

Compound	$g(1)$	$g(2)$	Reference
$[Fe_3(CO)_7L_2]^{\cdot -}$ [b]	2.048	2.002	this work
$[Fe_3(CO)_7L_2]^{\cdot +}$ [c]	2.050	2.002	this work
$[Fe_3(CO)_{12}]^{\cdot -}$	2.051	2.003	15
$[Fe_3(CO)_{11}P(OPh)]^{\cdot -}$	2.052	2.003	15
$[Fe_2(CO)_9]^{\cdot -}$	2.040	2.002	15

[a]Electrolysis was performed at −40 °C and ESR spectra were measured at −150 °C. [b]Electrolysis at −1.0 V. [c]Electrolysis at 1.15 V.

Electrolysis of $Fe_3(CO)_7L_2$ at +1.15 V produces an ESR signal which is very similar to that observed for electrolysis at −1.0 V. Comparable ESR signals have been obtained previously for reduction of $Fe_3(CO)_{12}$ and $Fe_3(CO)_{11}P(OPh)_3$ in tetrahydrofuran [15] and are shown in Table II.

ESR signals for the first reduction (wave II) as well as for first oxidation (wave I) are clearly indicative of anion and cation radical respectively [15]. The second reduction (wave III) also produces two ESR signals at $g = 2.039$ and 2.002. These values are close to that observed for the anion radical $Fe_2(CO)_9^{\cdot -}$ (Table II).

Mechanism of Reduction of $Fe_3(CO)_7L_2$

On the basis of the potentials of redox processes, electronic absorption spectra and ESR spectra, the first reduction of $Fe_3(CO)_7L_2$ may be postulated to produce the radical anion as shown in reaction (1).

$$Fe_3(CO)_7L_2 + e \underset{T < -10\,^\circ C}{\rightleftharpoons} [Fe_3(CO)_7L_2]^{\cdot-} \quad (1)$$

At low temperature, the $[Fe_3(CO)_7L_2]^{\cdot-}$ radical is stable and reaction (1) is reversible. The electrochemical reversibility of the reaction observed at low temperatures indicates the $Fe_3(CO)_7L_2$ framework remains intact in the radical which can be completely reoxidized to the original compound within the time scale (seconds) of the cyclic voltammetric measurement (wave II). At temperatures higher than -10 °C, the $[Fe_3(CO)_7L_2]^{\cdot-}$ radical undergoes partial decomposition with the product(s) of this reaction further reduced at more negative potential (wave III) in a one electron transfer process.

$[Fe_3(CO)_{12}]^{\cdot-}$ is formed in the one electron transfer reaction at 20 °C according to reaction (2)

$$Fe_3(CO)_{12} + e \rightleftharpoons [Fe_3(CO)_{12}]^{\cdot-} \quad (2)$$

In dichloromethane, chemical reversibility for electrode process (2) ($E_{1/2} = -0.21$ V *versus* Ag/AgCl) was observed at room temperature under cyclic voltammetric conditions with a scan rate of 0.2 V s^{-1} [15]. Thus, $Fe_3(CO)_{12}$ forms a radical anion that is reasonably stable on the electrochemical time scale. Under these same conditions, at room temperature, about 20% of $[Fe_3(CO)_7L_2]^{\cdot-}$ undergoes decomposition indicating the stability of $[Fe_3(CO)_7L_2]^{\cdot-}$ is less than the stability of $[Fe_3(CO)_{12}]^{\cdot-}$.

Substitution of carbonyl groups in $Fe_3(CO)_{12}$ by the basic ligand, α-diazothioketone in $Fe_3(CO)_7L_2$ progressively decreases the lifetime of the reduced product, with an accompanying significant (600 mV) cathodic shift in half-wave potential [16]. Theoretical calculations and arguments based on chemical and structural data suggest that both the HOMO and LUMO in the metal carbonyl cluster are predominantly metallic in character [16]. An increase in charge on the iron atoms brought about by substituting a basic ligand will increase the energy of the HOMO and reduction will be more difficult. This trend was observed previously for $Fe_3(CO)_{12-n}L'_n$ (where L' = phosphine ligand) [17].

At higher temperatures, the electrochemical reduction of $Fe_3(CO)_7L_2$ (peak II) becomes only quasireversible due to the decomposition of the radical anion produced

$$[Fe_3(CO)_7L_2] + e \underset{T > -10\,^\circ C}{\rightleftharpoons}$$

$$[Fe_3(CO)_7L_2]^{\cdot-} \xrightarrow{\text{fast}} \text{product(s)} \quad (3)$$

This is a typical EC type mechanism in which a chemical step follows an electrochemical reduction. In this case, a species is produced which is reduced in a one electron transfer reaction at a more negative potential than the parent compound (peak IIIc). Second reduction (peak IIIc) is irreversible in CH_2Cl_2 and CH_3CN but peak III'a obtained in cyclic voltammetry may be assigned to the oxidation of the product of electrochemical reduction (peak III) followed by a chemical step. Therefore, the overall process for wave II and III will proceed according to an ECEC mechanism.

The detailed nature of the product of decomposition of $[Fe_3(CO)_7L_2]^{\cdot-}$ is not clear. Half-wave potential, $E_{1/2} = -1.13$ V, for wave III is too positive to be assigned to the reduction of mono-iron species $Fe(CO)_{7-n}L'_n$. $E_{1/2}$ observed for the reduction of $Fe(CO)_5$ in acetone is -1.63 V *versus* SCE and substitution of organic ligand, L, to $Fe(CO)_5$ should shift this potential toward more negative potentials. UV–Vis spectra obtained after first reduction (Fig. 6) indicates the product of decomposition of the $[Fe_3(CO)_7L_2]^{\cdot-}$ radical still remains a triiron fragment.

According to earlier papers relating to electrochemistry of organometallic compounds regarding species of type RmQ (where R, Q = organic ligands or carbonyl; m = metal), there are several possible fates for the $RmQ^{\cdot-}$ species produced in a one electron transfer reduction process [16]. The first step in the decomposition of $RmQ^{\cdot-}$ produces Q^- and $Rm^{\cdot}$ followed by one or more pathways. These include mainly protonation, dimerization or generation of R·. Based on ESR data, one of the products of the second reduction of $[Fe_3(CO)_7L_2]$ can be tentatively assigned as $Fe_2(CO)_9^{\cdot-}$ (Table II).

Mechanism of Oxidation of $Fe_3(CO)_7L_2$

Voltammograms for $Fe_3(CO)_7L_2$ in non-aqueous solvents reveal irreversible and/or quasireversible oxidation waves which are dependent upon temperature and potential scan rate. Process reversibility is greater in non-coordinating solvents such as CH_2Cl_2 and at low temperatures. The reversible electrode process is the formation of cation radical

$$[Fe_3(CO)_7L_2] - e \rightleftharpoons [Fe_3(CO)_7L_2]^{\cdot+} \quad (4)$$

which is unstable; and, in the timescale of cyclic voltammetry, undergoes total decomposition at room temperature or partial decomposition at low temperature (Fig. 3). The product of decomposition retains a triiron framework in non-coordinating solvents *i.e.* CH_2Cl_2.

A cyclic voltammogram of $Fe_3(CO)_7L_2$ obtained in Me_2SO solution is shown in Fig. 7. Peaks I and II are similar to that observed in CH_2Cl_2 and CH_3CN. The reduction observed at peak IIIc which is observed to be an irreversible process in CH_2Cl_2 and CH_3CN is quasireversible in Me_2SO. Reversing the potential scan at potentials more positive than +0.8 V (process Ia) yields a new reduction peak at 0.26 V (IVc) with peak current about one third that observed for oxidation process Ia. At slow potential scan rates, (below 0.1 V s^{-1}), process IVc is reversible and an

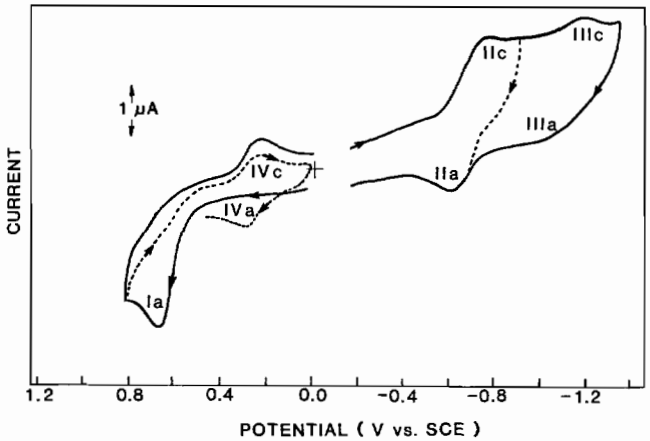

Fig. 7. Cyclic voltammogram of 1 mM $Fe_3(CO)_7L_2$ in Me_2SO (0.1 M TBAP).

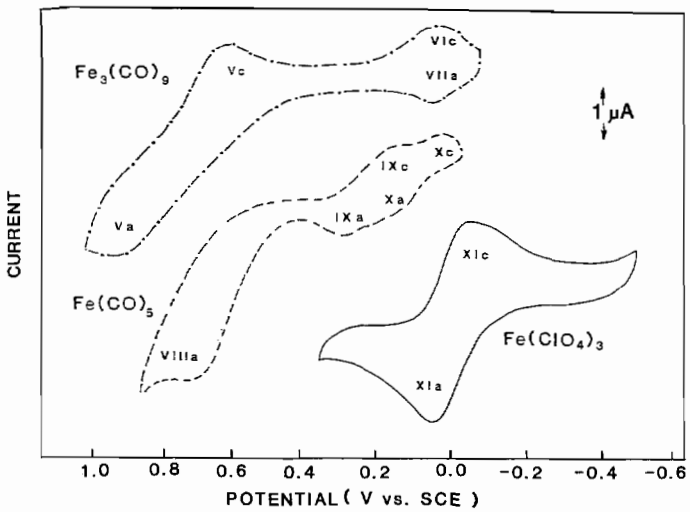

Fig. 8. Cyclic voltammograms of $Fe_3(CO)_9$ (– · –); $Fe(CO)_5$ (- - -); and $Fe(ClO_4)_3$ (——) in Me_2SO (0.1 M TBAP).

oxidation peak IVa can be observed at 0.20 V when the potential is reversed at 0.0 V. At higher potential scan rate, peak IVc decreases and a new peak at 0.22 V appears (peak IV′c not shown in Fig. 7).

In order to determine the origin of wave IVa, cyclic voltammograms of $Fe_3(CO)_9$, $Fe(CO)_5$ and $Fe(ClO_4)_3$ in Me_2SO were obtained (Fig. 8). Cyclic voltammograms show an oxidation peak at 0.9 V (peak Va) for $Fe_3(CO)_9$ and at 0.72 V (peak VIIIa) for $Fe(CO)_5$. Potential reversal at about 1.0 V produces an anodic peak Vc coupled to peak Va but no cathodic peak coupled to peak VIIIa. The current of peak Vc is about 30% lower than the current of anodic peak Va. This is very similar to analogous processes occurring with the triiron cluster in Me_2SO (peak Ic). In addition, one cathodic peak appears at potential 0.09 V for Fe_3CO_9. Again, it is a similar peak (with current about 30% of peak Va) to peak IVc; but the potential is shifted 170 mV in the negative direction. Cyclic voltammetry data indicate the cation radicals of the triiron complexes break apart and one of the products of fragmentation is a monoiron complex $Fe^{3+}(CO)_n(Me_2SO)_m$. The number of CO and Me_2SO ligands (n and m) will vary depending on the structure of the radical which undergoes decomposition $[Fe_3(CO)_7L_2]^{+\cdot}$ or $[Fe_3(CO)_9]^{+\cdot}$ and will influence the reduction potential of the complex fragment $Fe^{3+}(CO)_nMe_2SO_m$. The reduction of other products of fragmentation of triiron complexes, which presumably involves the diiron segment, is not observed in the range of potentials between 0.0 and 1.0 V. Decomposition of $[Fe(CO)_5]^{+\cdot}$ produces two $Fe^{3+}(CO)_nMe_2SO_m$ complexes with a different n/m ratio which is indicated by two reduction peaks at 0.20 and 0.08 V (peak IXc and Xc respectively). A cathodic peak XIc of the reduction of Fe^{3+} to Fe^{2+} in the absence of the CO ligand in Me_2SO is observed at 0.09 V. In coordinating solvents, like Me_2SO, results of cyclic voltammetry and spectroelectrochemistry indicate the

triiron structure of the triiron cluster is more destabilized and the cation radical $[Fe_3(CO)_7L_2]^{\ddagger}$ breaks apart

$$[Fe_3(CO)_7L_2]^{\ddagger} + Me_2SO \longrightarrow Fe^{+3}(CO)_n(Me_2SO)_m + Fe_2(CO)_{7-n}L_2(Me_2SO)_p \quad (5)$$

From the cyclic voltammetric data, it is quite clear that the Fe^{3+}/Fe^{2+} complex with solvent molecules is one of the products of decomposition of the $[Fe_3(CO)_7L_2]^{\ddagger}$ radical. Therefore, it is reasonable to assume that one Fe atom is separated from the original molecule while two other Fe atoms probably remain associated.

The previous work on the reduction and oxidation of $M(CO)_4L$ complexes, has suggested that the reduction is predominantly localized on the organic ligand, whereas the oxidation results in removal of one electron from orbitals predominantly of metal origin [16, 17]. For $Fe_3(CO)_7L_2$, labilization of ligand and change of coordination sphere are observed in the radical anion and cation formed in the electrochemical process. In the case of the cation, substitution proceeds via the solvent molecule, whereas the anion requires the action of a nucleophile. The rate of substitution is significantly higher in the cation radical than in the anion. A removal of one d electron from iron has a greater labilizing effect than addition of one electron into the ligand π system.

Regardless, stability of the radicals produced electrochemically is higher than might be expected for a linear rather than clustered triiron structure. Preservation of the Fe–Fe–Fe framework is observed to exist following formation of both the cation and anion radical in non-bonding solvents. Only strongly bonding solvents such as Me_2SO will break the structure.

Furthermore, lowering the temperature stabilizes both the anion and cation radical with the temperature necessary to achieve stabilization being relatively high (−10/−40 °C). Finally, although both the anion and cation radicals produced are stable, the cation radical is less stable and vulnerable to strongly bonding solvents.

These factors may be of significance in the application of these species as synthetic tools.

References

1 K. H. Pannell, Bansi Kalsotra and C. Parkanyi, *J. Heterocycl. Chem., 15,* 1057 (1978).
2 K. H. Pannell, A. J. Mayr, R. Hoggard and R. C. Pettersen, *Angew. Chem., Int. Ed., 19,* 632 (1980).
3 R. C. Pettersen, K. H. Pannell and A. J. Mayr, *Acta Crystallogr., Sect. B, 36,* 2434 (1980).
4 R. C. Pettersen, K. H. Pannell and A. J. Mayr, *Cryst. Struct. Commun., 9,* 643 (1980).
5 K. H. Pannell, A. J. Mayr, R. Hoggard, J. Dawson and J. McKennis, *Chem. Ber., 116,* 230 (1983).
6 K. H. Pannell, A. J. Mayr and D. VanDerveer, *Organometallics, 2,* 560 (1983).
7 K. H. Pannell, A. J. Mayr and D. VanDerveer, *J. Am. Chem. Soc., 105,* 6186 (1983).
8 K. H. Pannell, A. J. Mayr and B. Flores, unpublished results.
9 D. A. Hall and P. J. Elving, *Anal. Chim. Acta, 39,* 141 (1967).
10 J. Fajer, D. C. Borg, A. Forman, D. Dolphin and R. H. Felton, *J. Am. Chem. Soc., 92,* 3451 (1970).
11 R. K. Rhodes and K. M. Kadish, *Anal. Chem., 53,* 1539 (1981).
12 R. N. Bagchi, A. M. Bond and R. Colton, *J. Electroanal. Chem., 199,* 297 (1986).
13 Z. Galus, 'Fundamentals of Electrochemical Analysis', Ellis Horwood, U.K., 1976.
14 V. Gutman, 'The Donor–Acceptor Approach to Molecular Interactions', Plenum, New York, 1978.
15 B. M. Peake, B. H. Robinson, J. Simpson and D. J. Watson, *J. Chem. Soc., Chem. Commun.,* 945 (1974).
16 A. A. Vlcek, *Coord. Chem. Rev., 43,* 39 (1982), and refs. therein.
17 A. M. Bond, P. A. Dawson, B. M. Peake, B. H. Robinson and J. Simpson, *Inorg. Chem., 16,* 2199 (1977), and refs. therein.